Global and Planetary Change 122 (2014) 70–81

Contents lists available at ScienceDirect

Global and Planetary Change

journal homepage: www.elsevier.com/locate/gloplacha

Spatial variations of sea level along the coast of Thailand: Impacts of extreme land subsidence, earthquakes and the seasonal monsoon

Suriyan Saramul [a], Tal Ezer [b,*]

[a] Department of Marine Science, Faculty of Science, Chulalongkorn University, Phyathai Road, Pathumwan, Bangkok 10330, Thailand
[b] Center for Coastal Physical Oceanography, Old Dominion University, 4111 Monarch Way, Norfolk, VA 23508, USA

ARTICLE INFO

Article history:
Received 2 April 2014
Received in revised form 9 August 2014
Accepted 11 August 2014
Available online 19 August 2014

Keywords:
sea level rise
seasonal sea level cycle
Gulf of Thailand
Andaman Sea
Sumatra Earthquake

ABSTRACT

The study addresses two important issues associated with sea level along the coasts of Thailand: first, the fast sea level rise and its spatial variation, and second, the monsoonal-driven seasonal variations in sea level. Tide gauge data that are more extensive than in past studies were obtained from several different local and global sources, and relative sea level rise (RSLR) rates were obtained from two different methods, linear regressions and non-linear Empirical Mode Decomposition/Hilbert–Huang Transform (EMD/HHT) analysis. The results show extremely large spatial variations in RSLR, with rates varying from ~1 mm y^{-1} to ~20 mm y^{-1}; the maximum RSLR is found in the upper Gulf of Thailand (GOT) near Bangkok, where local land subsidence due to groundwater extraction dominates the trend. Furthermore, there are indications that RSLR rates increased significantly in all locations after the 2004 Sumatra–Andaman Earthquake and the Indian Ocean tsunami that followed, so that recent RSLR rates seem to have less spatial differences than in the past, but with high rates of ~20–30 mm y^{-1} almost everywhere. The seasonal sea level cycle was found to be very different between stations in the GOT, which have minimum sea level in June–July, and stations in the Andaman Sea, which have minimum sea level in February. The seasonal sea-level variations in the GOT are driven mostly by large-scale wind-driven set-up/set-down processes associated with the seasonal monsoon and have amplitudes about ten times larger than either typical steric changes at those latitudes or astronomical annual tides.

1. Introduction

The coasts of Thailand include three different regimes. In the north are the coasts surrounding the shallow estuarine-like system (centered at ~13°N; Fig. 1) known as the Upper Gulf of Thailand, with circulation driven by tides, river runoffs and the seasonal monsoonal winds (Saramul and Ezer, 2014). The two coasts in the south include the eastern coast located on the western side of the Gulf of Thailand (GOT) which is connected through the South China Sea to the Pacific Ocean, while the western coast is along the Andaman Sea, which is connected to the Indian Ocean (Fig. 1). Therefore, different coastal ocean dynamics may be expected at each of these regions. In the GOT, the topography is relatively shallow (average depth of approximately 45 m in the entire GOT, and ~15 m in the upper GOT); and tides are the result of two tidal waves that move in opposite directions, one coming from the South China Sea along the east coast and another one from a reflected tide in the GOT itself (Wyrtki, 1961; Fuh, 1977). On the other hand, the Andaman Sea was formed and influenced by a chain of volcanic activities, so the bottom topography changes rapidly from deep regions, ~2500 m, in the center of the Sea to ~200 m near islands and coasts; internal waves are thus often observed in this region (Rizal et al., 2012; Yi-Neng et al., 2012).

Tides in the GOT are found to be both mixed and diurnal depending on geographic location with typical tidal ranges of 1–3 m (Saramul, 2013). Unlike the GOT, tides in the Andaman Sea are mainly semi-diurnal with range of ~3 m along the coast of Thailand (Brown, 2007). The combined impact of tides, storm surge from typhoons, monsoonal floods and sea level rise can severely impact lives and properties of coastal communities (Douglas, 2001). The global rate of mean sea level rise (GSLR) based on more than 100 years of tide gauge data is around 1.7 ± 0.3 mm y^{-1}, compared to sea level rise of about 3.2 ± 0.5 mm y^{-1} obtained from ~20 years of satellite altimeter data (Church and White, 2006, 2011). The differences between the tide gauge and satellite data has been attributed to global sea level acceleration (Church and White, 2011), spatial location of tide gauges and satellite observations (Dean and Houston, 2013) and multi-decadal variations not captured by the shorter altimeter data (Ezer, 2013). However, for coastal communities under flooding threat, GSLR may not be as important as local RSLR. For example, large spatial variations in RSLR in places such as the U.S. East Coast are due to land subsidence and changes in the Gulf Stream and other ocean currents (Ezer and Corlett, 2012; Sallenger et al., 2012; Ezer, 2013; Ezer et al., 2013; Kopp, 2013). The results presented here will show that spatial variations in RSLR along

* Corresponding author.
E-mail address: tezer@odu.edu (T. Ezer).

http://dx.doi.org/10.1016/j.gloplacha.2014.08.012
0921-8181/

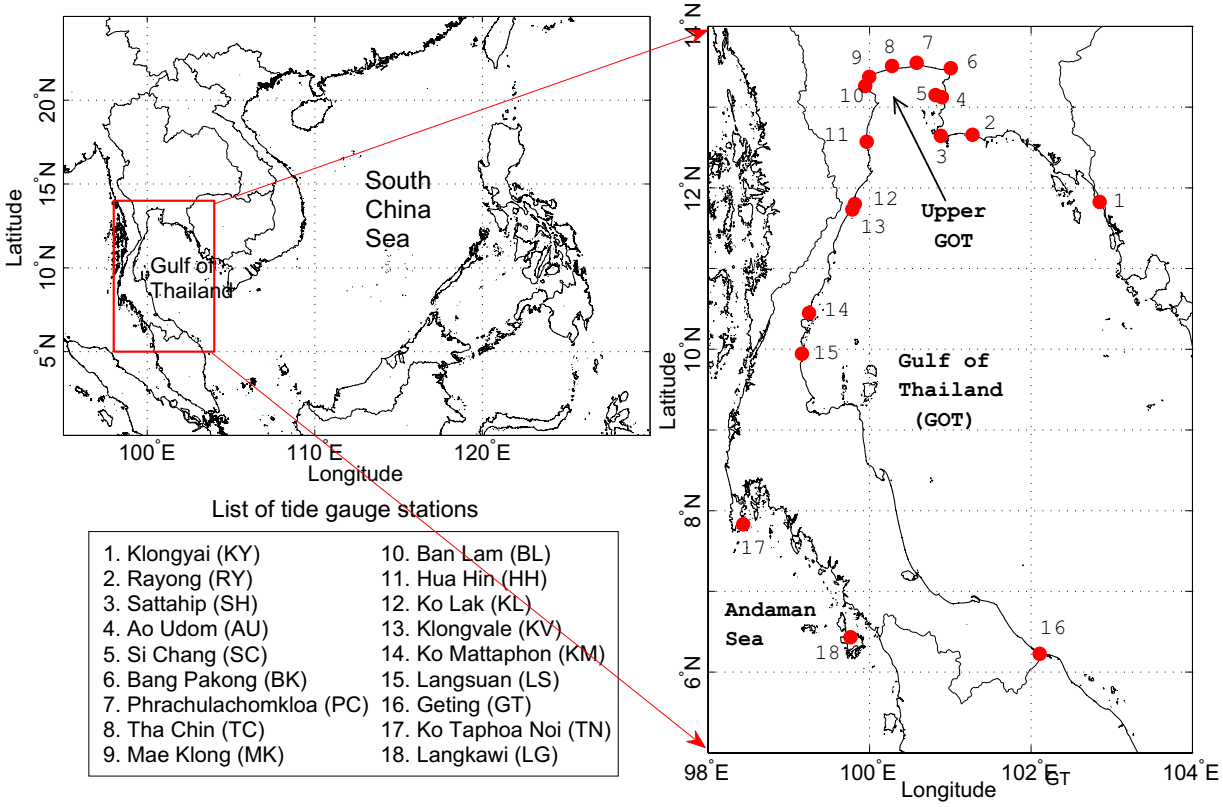

Fig. 1. Map of the study area and locations of 18 tide gauge stations in the GOT and Andaman Sea used in the study.

the coast of Thailand are much larger than even those recently reported for the U.S. coasts.

There are only sparse studies of sea level rise in Thailand and they are often contradicting each other due to sparsely observed coastal sea level and gappy data. For example, Yanagi and Akaki (1994) studied sea level variability in Eastern Asia during 1951–1991 using data obtained from the Permanent Service for Mean Sea Level (PSMSL) and found a rate of sea level rise as high as 16.4 ± 0.85 mm y^{-1} at Phrachulachomkloa, in the upper GOT, but rates close to the GSLR, 2.3 ± 1.1 mm y^{-1}, at Taphoa Noi, in the Andaman Sea (see Fig. 1 for locations). However, in some locations large discrepancies in RSLR were reported by different studies. In Si Chang, reported sea level rise was 0.6 ± 0.39 mm y^{-1} for 1951–1991 (Yanagi and Akaki, 1994), but -0.36 mm y^{-1} for 1940–1996 (Vongvisessomjai, 2006, 2010). In Ko Lak, a reported sea level downward trend was -0.83 ± 0.22 mm y^{-1} for 1951–1991 (Yanagi and Akaki, 1994), -0.36 mm y^{-1} for 1940–1996 (Vongvisessomjai, 2006, 2010), but -6.25 mm y^{-1} for 1988–2006 (Siwapornnanan et al., 2011). Even though the distance between Ko Lak and Si Chang is only 150 km apart, with presumably similar oceanographic, meteorological, and tectonic conditions, it is not clear why the stations have an opposite sea level trend. Recent studies of sea level in the GOT that include GPS measurement to correct land movements still found that the rate of sea level rise in the area, 3.0–5.5 mm y^{-1}, is significantly faster than the GSLR (Trisirisatayawong et al., 2011); unlike the earlier studies mentioned before, this latest study indicates a rising sea level rate of 3.6 ± 0.7 mm y^{-1} at Ko Lak (i.e., absolute rate). Another recent study of sea level variations in the GOT (Oliver, 2014), used tide gauge data for 1985–2010, and a numerical ocean circulation model, to show the importance of the intraseasonal, wind-driven variations associated with the Madden–Julian Oscillation (MJO); the latter study includes 2 of the tide gauges used here, but none was located in the upper GOT.

These conflicting and confusing results, and the importance of sea level rise in this region, motivated this new analysis of sea level, which includes a larger set of sea level data than most previous studies. Because of the possible non-linear nature of the RSLR in this region, two methods are used to estimate trends, a standard linear least-square fit and a non-linear non-parametric method based on Empirical Mode Decomposition (Huang et al., 1998). The latter method, which filters oscillatory modes from the trend, has been recently adapted to sea level studies (Ezer and Corlett, 2012; Ezer, 2013; Ezer et al., 2013). While land movement due to Glacial Isostatic Adjustment (GIA; Peltier, 2004) is very small in the study area and is almost linear, a non-linear sea level rise in the GOT's region may be attributed to earthquakes and increased groundwater extraction near Bangkok, Thailand (Nicholls, 2011). Geological studies show that past earthquakes had impact on RSLR rates in the Sumatra region due to vertical tectonic motion (Dura et al., 2011). For example, Sieh et al. (2008) show that over the past 700 years there were several earthquakes in this region; land uplift occurred during almost every one of them, which followed by gradual subsidence. While detailed geological survey of the impact of earthquakes on the region is beyond the scope of this study, the possible impacts on sea level from the December 26, 2004, Sumatra–Andaman Earthquake are evaluated; note that the tsunami that follows the earthquake also caused considerable damage and changes in the coasts of Thailand.

An important component of sea level variability is the seasonal cycle, which may be driven by meteorological and oceanographic processes, such as wind, atmospheric pressure, thermal steric effects, long-term astronomical cycles, as well as river runoffs (Gill and Niiler, 1973; Tsimplis and Woodworth, 1994; Torres and Tsimplis, 2012). However, very little is known on the seasonal sea level variations around Thailand and their forcing mechanisms. For example, Tsimplis and Woodworth (1994), analyzed only 3 tide gauge stations in the GOT, compared with 14 tide gauge stations in both, GOT and Andaman Sea, analyzed here. Because of the scarcity of direct observations in the GOT, numerical ocean circulation models are often used to study seasonal variations in the region. For example, Wu et al. (1998) used a regional

model of the South China Sea and the GOT, Aschariyaphotha et al. (2008) used an ocean model with a curvilinear grid (grid size ~2–55 km) covering most of the GOT north of 6°N, and more recently, Saramul and Ezer (2014) used a high-resolution model (grid size ~1 km) covering only the upper GOT north of 12.5°N. All the above model results found that the dynamics of the region is dominated and driven by the seasonal monsoonal winds, which can reverse the circulation patterns obtained at different times of the year. Note also that other semi-enclosed shallow basins in low latitudes, even in the southern hemisphere, such as the Gulf of Carpentaria (Forbes and Church, 1983; Oliver and Thompson, 2010), have similar dynamics with strong seasonality driven by variations in the wind, atmospheric pressure and steric effects. Oliver (2014) used 6 tide gauges in the GOT, together with an ocean model, to show how wind-driven setup of sea level is affecting intraseasonal variations and how these variations are modulated by the seasonal monsoonal winds. We will thus investigate here how similarly wind-driven sea level setup may affect seasonal variations in sea level along the coasts of Thailand. It has been recognized that the coastal dynamics of this region is largely affected by the seasonal cycle in monsoonal winds, cloudiness and precipitation (Saramul and Ezer, 2014), but the exact mechanism and amplitude of the monsoonal impact on sea level need further research, given the limited data available in some past studies. Therefore, seasonal variations in sea level are analyzed, and in particular, comparisons are made between Thailand's coasts located on the GOT's side versus those located on the Andaman Sea's side; these two coasts are affected by a similar atmospheric forcing, but possibly different oceanic dynamics.

The paper is organized as follows. First, sources of sea level data and the analysis methods are described in Section 2. Second, results of sea level analysis are discussed in Section 3, looking at spatial variations in RSLR and then on the seasonal cycle and it's forcing. Finally, summary and conclusions are offered in Section 4.

2. Data and methodology

There are approximately 27 tide gauge stations operated in Thai Waters (both in the GOT and Andaman Sea). Based on availability and data quality, only 18 tide gauge station will be analyzed in this paper (Figs. 1 and 2). The data are obtained from 4 sources, which are Thailand's Marine Department (MD), Hydrographic Department (HD), Permanent Service for Mean Sea Level (PSMSL; http://www.psmsl.org/) (Woodworth and Player, 2003; Holgate et al., 2013), and the University of Hawaii Sea Level Center (UHSLC; http://uhslc.soest.hawaii.edu/ and http://ilikai.soest.hawaii.edu/). PSMSL provides only monthly and annual mean sea level, while other sources also provide hourly or daily data, so here only monthly averaged data are analyzed for all stations. The periods of available data from these 4 sources are different for each station (Fig. 2), with the longest records, ~70 years, at Ko Lak, Ko Taphoa Noi and Phrachulachomkloa stations.

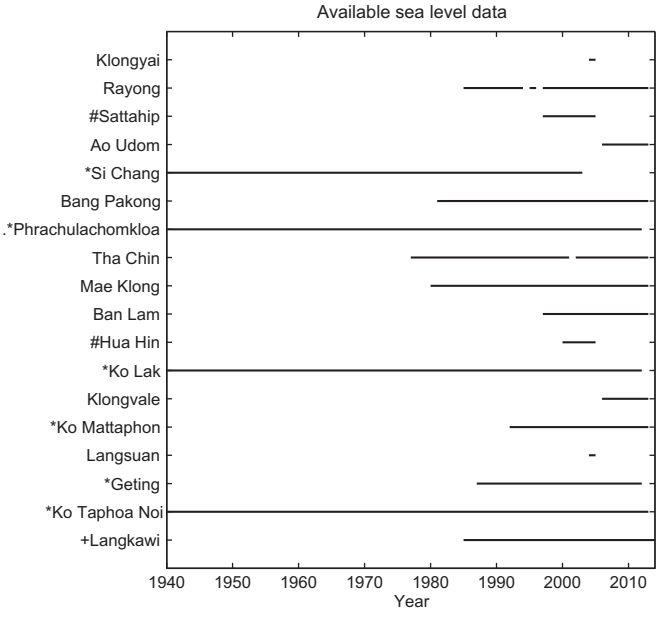

Fig. 2. The period and source of sea level data used in this study. Sea level data are obtained from Marine Department (no mark), Hydrographic Department (#), Permanent Service for Mean Sea Level (*), and the University of Hawaii Sea Level Center (+).

The mean RSLR rate is calculated for stations that have at least 15 years of data. This estimated rate includes the impact of vertical land movement due to seismic activity/glacial rebound and anthropogenic activity. The monthly mean sea level data analyzed for all stations eliminates tides and high-frequency variations (no other tidal filtering is done). Two analysis methods are used: 1) least square linear fit and 2) an averaged slope estimated from the trend which is the last one or two modes of Empirical Mode Decomposition and Hilbert–Huang Transform (EMD/HHT) (Huang et al., 1998). The EMD/HHT method can be used to separate oscillatory modes on various scales (e.g., tides, seasonal, and interannual) from long-term trends, and applies to any non-stationary or nonlinear time series. The method produces mean sea level trend and sea level acceleration comparable to linear and polynomial least-square fits; bootstrap simulations can also be used to obtain error estimates (Ezer and Corlett, 2012). This method has been applied for sea level data in the Chesapeake Bay (Ezer and Corlett, 2012), the mid-Atlantic Bight (Ezer et al., 2013) and the entire U.S. East coast (Ezer, 2013). When compared with the linear trend, the EMD trend can show if the rate of sea level changes with time, i.e., if there is acceleration or deceleration of sea level rise (Ezer, 2013).

Estimated errors in tide gauge data follow standard sea level analysis procedures (Jevrejeva et al., 2006). The error of mean sea level caused by inverted barometer is neglected here since it has a minimal impact in this region (Punpuk, 1981), and many stations do not provide such information. Glacial Isostatic Adjustment (GIA) corrections (Peltier, 2004; ICE-5G-VM2 model, updated 2012) are taken into account. Unfortunately, not all tide gauge stations have the value of GIA corrections. Therefore, the station that has no GIA correction will use the one from stations nearby (within 100 km). If there are no stations nearby, interpolation from station within 1000 km will be applied. Note, however, that vertical land movement due to groundwater withdrawal, earthquakes, and other processes are significantly larger than GIA in the GOT and Andaman Sea regions, therefore local land movements other than GIA is included in the sea level rise calculations. The mean linear trend and 95% confidence interval are calculated from standard least-square fitting while the mean trend of the EMD/HHT is calculated from the mean slope of the (non-linear) trend which is the residual after all oscillating modes are removed (Huang et al., 1998). Estimating errors and confidence intervals over the mean rate in EMD/HHT is more complex and can be done in various ways. Here, following Ezer and Corlett (2012), bootstrap simulations (randomly re-sampling the anomaly) were conducted with varies record lengths and various number of ensemble members. Based on these experiments, and considering the EMD/HHT and other data errors, for record of Y years an empirical relation was used for the 95% confidence interval, $\pm$CI (mm y^{-1}) = max (0.575–0.0075 Y, 0.1). The CI of the EMD/HHT is usually smaller than linear regression since the method systematically removes all high-frequency oscillations, as well as interannual variations from the trend. While the error estimates relative to the mean in the two methods cannot be directly compared, the main purpose of using two different methods is to see if similar spatial pattern in RSLR is seen and to possibly identify non-linear trends not captured by the linear regression method.

3. Results and discussions

3.1. Spatial pattern of sea level rise rates

Monthly mean sea level variability and trends at 8 tide gauge stations along the coasts of the GOT and Andaman Sea are shown in Fig. 3 (the last two stations shown, Ko Taphoa Noi and Langkawi are the only ones from the Andaman Sea). While the linear trends and the non-linear EMD trends seem very similar for most stations, the EMD trend can indicate some departure from linear sea level rise. For example, in Phrachulachomkloa positive sea level acceleration at the beginning of the record may relate to increased groundwater extractions near Bangkok in the 1960s (Nicholls, 2011), while in Ko Taphoa Noi the positive sea level acceleration near the end of the record may relate to its proximity to the epicenter of the 2004 Sumatra–Andaman Earthquake. It is also quite clear that sea level rise rates in the upper GOT (Phrachulachomkloa and Mae Klong) are larger than in other locations. Interestingly enough, the RSLR rate at Si Chang (also located in the upper GOT, but on the eastern shore) is quite low, which is consistent with results from Yanagi and Akaki (1994) and Vongvisessomjai (2006, 2010), who show small positive and small negative rates, respectively. The large spatial difference in RSLR between Si Chang and nearby stations will be discussed later.

The sea level rise rates are summarized in Fig. 4a and Table 1. In general, there are three categories of stations: in the north, very large RSLR rates are seen, in the South (Geting, Ko Taphoa Noi, and Langkawi), small positive rates similar to the GSLR are seen, and two stations (Si Chang and Ko Lak), show nearly no significant RSLR. The numbers shown in Fig. 4a and Table 1 are the relative rates (without any corrections), and GIA is small here (Table 1). Note that the global averaged rate of sea level rise due to GIA is approximately -0.3 mm y^{-1} (Peltier, 2001; Peltier and Luthcke, 2009). Overall, the average rate of sea level rise in the GOT and Andaman Sea is larger than the global rate, but the most significant result is the spatial pattern seen in Fig. 4a (note that the order of stations are generally counter clockwise from the northeast on the left of Fig. 4 to the southwest on the right of Fig. 4). The differences in RSLR rates along ~1000 km of Thailand's coasts are as large as a factor of 10 between stations; in comparisons, RSLR rate differences along ~2000 km of the U.S. East Coast are about a factor of 2–3 between stations (Ezer, 2013).

In some stations, the difference rate between linear and EMD calculations is more than 50%, for example, in Bang Pakong and Ban Lam. However, these stations have relatively short records or they show rates that do not seem to be constant, thus a linear trend may not accurately represent the long-term sea level change if significant decadal variations that are not fully resolved exist (Ezer, 2013). In general, the same spatial pattern of RSLR is seen in both analysis methods (Fig. 4a) which shows that this pattern is robust. The EMD analysis also indicates positive RSLR acceleration on the north shores of the upper GOT which relates to land subsidence around Bangkok as discussed next.

3.2. Land subsidence and the 2004 Sumatra–Andaman Earthquake

As mentioned above, the rate of sea level rise found at Phrachulachomkloa, Tha Chin, Mae Klong, and Ban Lam is much higher than the global rate (approximately 5 times larger). Syvitski et al. (2009) also mentioned that Choa Phraya River Delta has the relative rate of sea level rise approximately 13–150 mm y^{-1}; note however, that such extremely high RSLR of 150 mm y^{-1} is very rare and has not been reported before. The fact that the land is sinking in the upper GOT (Bangkok and surrounded area) due to groundwater withdrawal is well known (Poland, 1984; Therakomen, 2001; Phien-Wej et al., 2006; Aobpaet et al., 2009; Nicholls, 2011), though the exact rates of land subsidence is not easily measured. Groundwater extraction is considered an anthropogenic change in sea level, but globally typical rates of such land subsidence are ~0.1–0.3 mm y^{-1} (Gornitz, 2001), thus much smaller than the land subsidence seen here. Groundwater has been pumped out in Bangkok and surrounded area and it has been recognized to cause land subsidence for the past 40 years or so. A sinking rate larger than 120 mm y^{-1} was found in the 1980s at central Bangkok, but it has been reduced to approximately 10 mm y^{-1} in the 2000s (Fig. 7 in Phien-Wej et al., 2006). In a recent study by

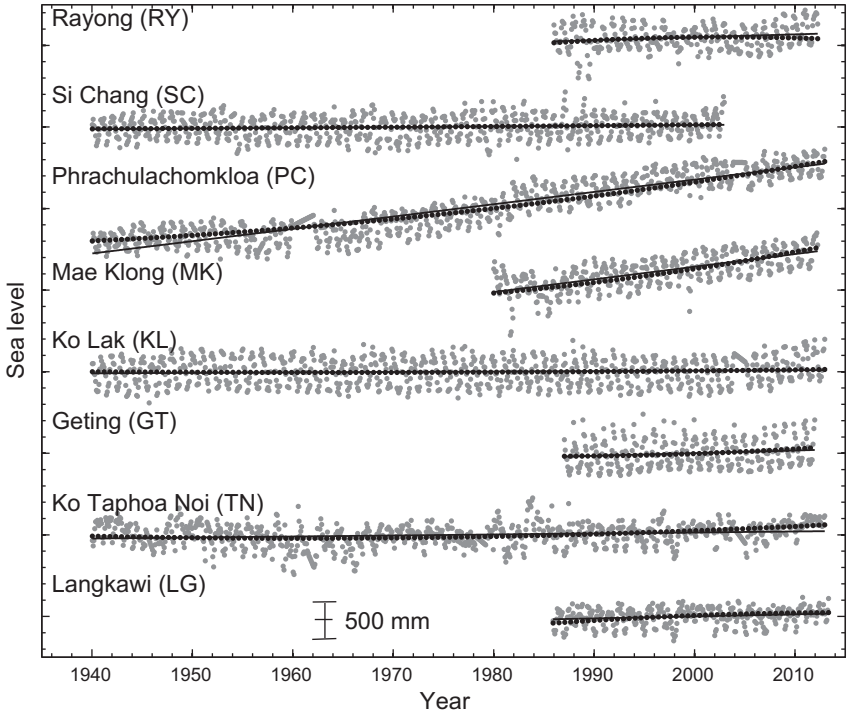

Fig. 3. Monthly sea level (gray dots) in the GOT (the first six stations) and Andaman Sea (the last two stations). Black solid line and black dot line represent linear and HHT trends obtained from linear fit and HHT/EMD analysis, respectively. Sea level scale is shown at the bottom.

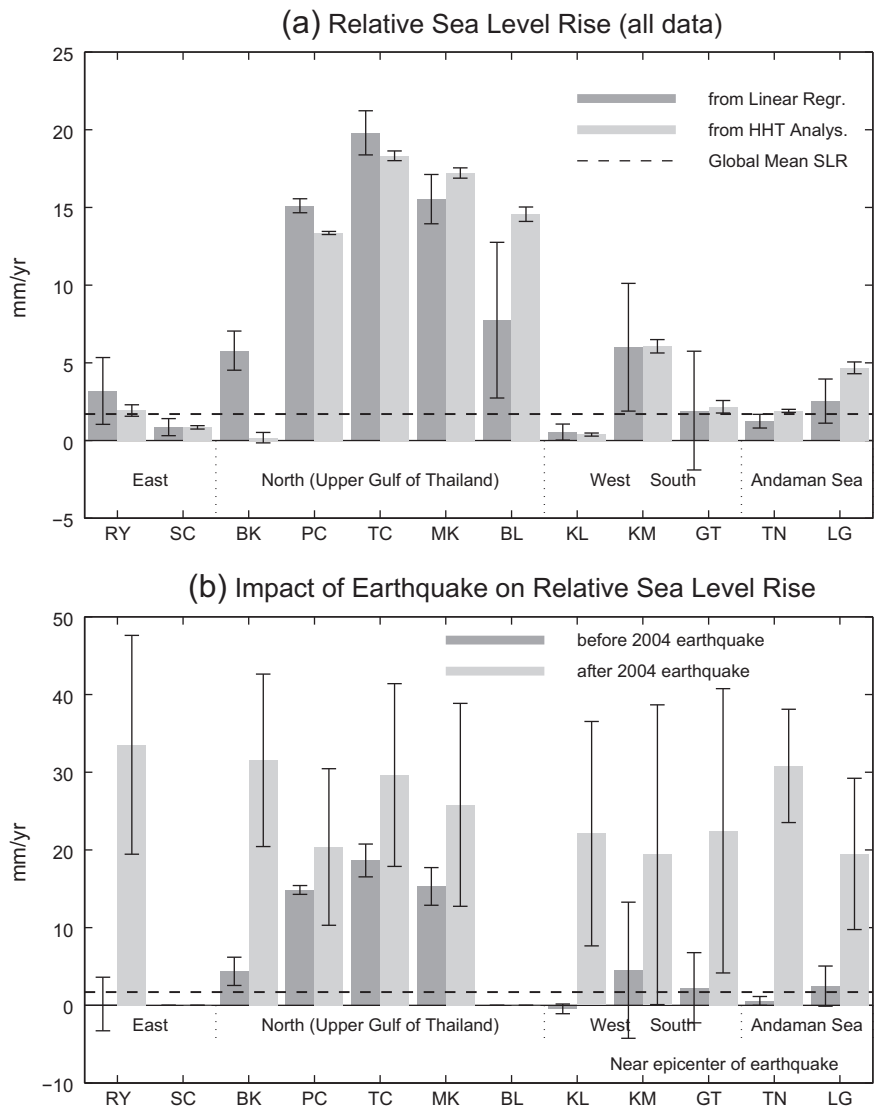

Fig. 4. (a) Rate of relative sea level rise ±95% confidence intervals based on linear fit of all available monthly mean sea level (dark gray) and slope of HHT trend analysis (light gray). Dashed line denotes global mean rate of sea level rise of 1.7 ± 0.3 mm y^{-1} (Church and White, 2006). The full names and locations of the stations are shown in Fig. 1. (b) Rates of relative sea level rise before (dark gray) and after (light gray) the 2004 Sumatra Earthquake. Two stations have gaps in data that do not allow these calculations. The stations closest to the epicenter of the earthquake are indicated.

Table 1
Rate of relative sea level rise and 95% confidence interval at each tide gauge station in the GOT and Andaman Sea. The rates are obtained from linear fit and HHT/EMD (slope of the trend represented by last modes). GIA corrections at each station are also shown (Peltier and Luthcke, 2009).

Station	Linear trend	HHT trend	GIA
Gulf of Thailand			
Rayong (RY)	3.19 ± 2.15	1.93 ± 0.37	−0.38
Si Chang (SC)	0.86 ± 0.55	0.84 ± 0.11	−0.38
Bang Pakong (BK)	5.78 ± 1.26	0.18 ± 0.34	−0.38
Phrachulachomkloa (PC)	15.10 ± 0.45	13.35 ± 0.10	−0.39
Tha Chin (TC)	19.80 ± 1.42	18.32 ± 0.31	−0.39
Mae Klong (MK)	15.53 ± 1.59	17.21 ± 0.33	−0.39
Ban Lam (BL)	7.74 ± 5.01	14.56 ± 0.46	−0.39
Ko Lak (KL)	0.54 ± 0.52	0.38 ± 0.10	−0.36
Ko Mattaphon (KM)	6.00 ± 4.11	6.06 ± 0.43	−0.34
getting (GT)	1.92 ± 3.82	2.17 ± 0.40	−0.33
Andaman Sea			
Ko Taphoa Noi (TN)	1.24 ± 0.44	1.90 ± 0.10	−0.28
Langkawi (LG)	2.53 ± 1.42	4.67 ± 0.38	−0.36

Aobpaet et al. (2009), interferometric synthetic aperture radar (InSAR), a SAR technique to detect the land movement, found that the eastern central Bangkok area still sinking with the rate of ~15 mm y^{-1}. Since Phrachulachomkloa, Tha Chin, and Mae Klong stations are situated in the area where the land subsidence is still a problem, a faster rate of RSLR is expected and our calculations are consistent with land subsidence of 10–20 mm y^{-1}. Even after exclusion of tide gauge stations in the area of significant land subsidence and the correction using precise GPS technique has been applied, the average rates of sea level rise in the GOT is still faster than the global rate (Trisirisatayawong et al., 2011); the latter study also mentioned possible vertical land uplift due to the 2004 Indian Ocean Tsunami and the 2004 Sumatra–Andaman Earthquake. GPS measurements after the 2004 Sumatra–Andaman Earthquake show that many parts of Thailand are sinking at rates up to 10 mm y^{-1}. However, some projections of land subsidence for the next two decades in Bangkok area are estimated to be not more than 5 mm y^{-1} (Satirapod et al., 2013). Note that the area that has shown sinking, as mentioned above, extends approximately 650–1500 km away from the epicenter of the earthquake that caused the tsunami.

The impact of the 2004 earthquake on RSLR rates is shown in Fig. 4b, indicating that stations closer to the earthquake epicenter experienced the largest change in RSLR. Our results are quite consistent with other studies, but provide much more details. The vertical uplifts shown before the 2004 Sumatra–Andaman Earthquake (between 1994 and 2004) at GPS stations near Si Chang and Ko Mattaphon tide gauge stations are 2.2 ± 0.8 and 3.8 ± 1.3 mm y^{-1}, respectively. However after the earthquake (between 2004 and 2009), the land has been submerging at a rate of −12.7 ± 4.2 and −3.9 ± 2.1 mm y^{-1} at GPS stations near Si Chang and Ko Mattaphon, respectively (Trisirisatayawong et al., 2011). This means that not only the rate of sea level rise in Thailand has to be corrected by GIA corrections but also by vertical movement of the land due to seismic activity. Due to the lack of GPS stations data near other tide gauge stations, the pre- and post-2004 Sumatra–Andaman Earthquake rate of sea level rise in the GOT and Andaman Sea will be shown without any corrections and the results are presented in Figs. 5 and 6. Note that error bars in Fig. 4b are much larger after 2004 due to the shorter record. Before the 2004 earthquake, the relative rate of sea level rise in the GOT and Andaman Sea is gradually increasing in most stations, except at Ko Lak (Fig. 6) where the relative rate of sea level is falling, which is consistent with previous studies (Yanagi and Akaki, 1994; Vongvisessomjai, 2006, 2010). The relative rate of sea level rise at stations situated in the subsidence zone (i.e., Tha Chin, Mae Klong, and Phrachulachomkloa) was high, ~15–19 mm y^{-1}, even before the earthquake, and rates increased to ~20–30 mm y^{-1} after 2004. A more dramatic result is that after 2004 all 10 stations shown in Figs. 4b, 5 and 6 have very high RSLR in the range of 19–33 mm y^{-1}. Recent studies suggest that in addition to land subsidence that followed the earthquake, the land now continues to sink due to seismic activity (Trisirisatayawong et al., 2011; Satirapod et al., 2013). Our results indicate a significant shift in the spatial pattern, whereas before the 2004 earthquake there were very large (and statistically distinct; Fig. 4a) differences in RSLR due to local groundwater extraction in the north, but after the earthquakes (Fig. 4b), similarly large RSLR rates are found everywhere, with no statistically significant differences in RSLR between stations. One must be cautious though about the statistical confidence of the short records after 2004, so longer future records are needed in order to confirm if this trend is real and continues. The fact that RSLR rates after the earthquake are rising almost evenly everywhere regardless of distance from the earthquake's epicenter suggests that a large-scale vertical land movement due to seismic activity may be at play after the earthquake. Note that one of the largest increases in RSLR rate after the earthquake (from ~0.6 to ~31 mm y^{-1}) is found at Taphoa Noi (TN in Fig. 4b) which is the closest station to the earthquake's epicenter.

The vertical land motion after the 2004 earthquake is consistent with geological studies that indicate changes in RSLR, following other earthquakes in the Sumatra region over the past 4000 years (Dura et al., 2011). Fig. 7 shows the latest observations of vertical land movement in central Bangkok for 2009–2013 (i.e., after the 2004 earthquake), obtained from the global GPS network of the Nevada Geodetic Laboratory (geodesy.unr.edu); the rate of land sinking there is ~4 mm y^{-1}. This location is about 30 km north of the northern coast of the upper GOT, so it is possible that sinking rates are larger along the coast and in river deltas, as indicated by our analysis.

3.3. Seasonal sea level cycle

Besides tides, the seasonal cycle of sea level is often accounts for a large part of the variability (Tsimplis and Woodworth, 1994; Torres and Tsimplis, 2012). However, different regions may be affected by different oceanographic and meteorological forcing such as atmospheric pressure, winds and thermohaline steric effects (Gill and Niiler, 1973).

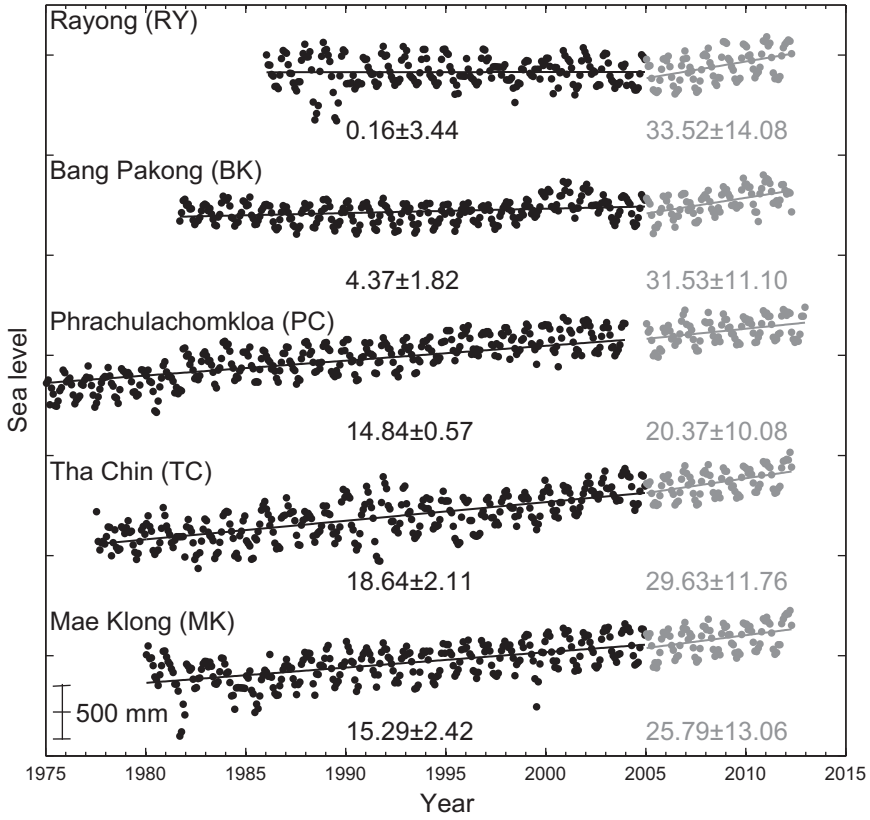

Fig. 5. Monthly mean sea level at each tide gauge station. Black and gray dots represent pre- and post-2004 Sumatra–Andaman Earthquake event, respectively. The linear trend is shown by the solid line and the rate of relative sea level rise (mm y^{-1} ± 95% confidence level) is indicated for each station. The stations situated in the upper GOT where the land subsidence is active are Bang Pakong, Phrachulachomkloa, Tha Chin, and Mae Klong.

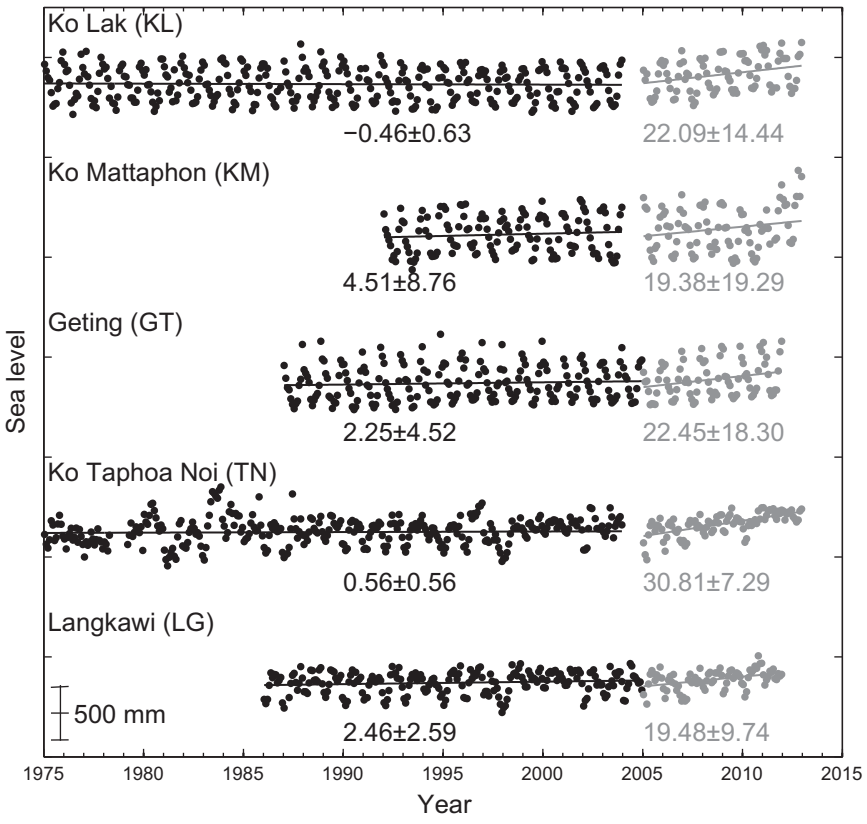

Fig. 6. Same as Fig. 5, but for stations in the south of the GOT and in the Andaman Sea.

In Thailand, previous studies of seasonal variations in sea level are sparse. For example, Tsimplis and Woodworth (1994) used only 3 tide gauge stations in the GOT (compared with 14 tide gauge stations situated in the GOT and the Andaman Sea, analyzed here). Understanding the seasonal variations is important for Thailand since coastal risk assessments may need to include seasonal variations when considering other risks such as sea level rise (discussed in the previous session), storm surges and monsoonal floods during the wet season. Various numerical ocean circulation models show that wind-driven variations in sea level and circulation patterns in the GOT are dominated by the seasonal monsoon (Wu et al., 1998; Aschariyaphotha et al., 2008; Saramul and Ezer, 2014). However, the extended sea level data used here can be used to verify the model results and compare the wind-driven component with other influences, such as the seasonal steric effect and the annual and semi-annual astronomical forcing.

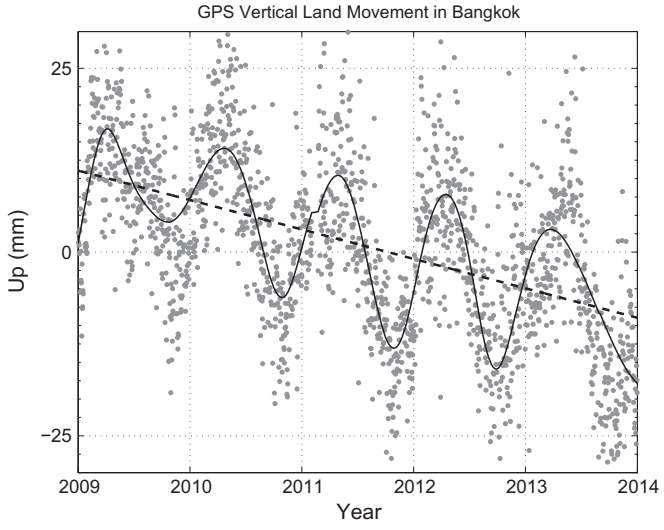

Fig. 7. GPS measurements of vertical land movement from central Bangkok (CUSV station, 13.736°N, 100.534°E; about 30 km north of the coast of the upper GOT) obtained from the Nevada Geodetic Laboratory (geodesy.unr.edu). Solid line is a smooth fit showing the seasonal cycle and dash line is the linear trend for 2009–2013 (-4 mm y^{-1}).

One of the forcing mechanisms of seasonal sea level change is due to the gravitational potential, associated with two long-period astronomical tidal harmonic components, the annual (S_a) and semi-annual (S_{sa}) components. Annual component accounts for the changing distance between the sun and the earth, while semi-annual component accounts for the changing solar declination (Torres and Tsimplis, 2012). These two components can be estimated from harmonic analysis, but one should keep in mind that such an analysis does not distinguish between astronomical forcing and other forces (in particular, wind-driven as discussed later). Linear regression least-square fit methods will be used to fit monthly mean sea level anomaly of month i ($\overline{M}_i$) following Tsimplis and Woodworth (1994),

$$\overline{M}_i = A_{Sa}\cos\left[\frac{\pi}{6}(t-\varnothing_{Sa})\right] + A_{Ssa}\cos\left[\frac{\pi}{3}(t-\varnothing_{Ssa})\right] \quad (1)$$

where A_{Sa} and A_{Ssa} are the amplitudes and $\varnothing_{Sa}$ and $\varnothing_{Ssa}$ are the phases of the annual and semi-annual components. Note that the equilibrium global amplitude of these long tidal constituents are $A_{Sa} \approx 3$ mm and $A_{Ssa} \approx 19$ mm, but are these values consistent with the observed seasonal changes along the Thailand's coasts?, the results below show much larger variations on those periods. The time, t, is taken in the

middle of each month i ($t = i - 0.5$). $\overline{M}_i$ is estimated from averaging monthly sea level anomaly, M_{ik} (a deviation of month i from annual mean of year k), over N_{yr}. Therefore mean monthly sea level anomaly can be expressed as

$$\overline{M}_i = \frac{1}{N_{yr}} \sum_{k=1}^{N_{yr}} M_{ik}. \quad (2)$$

As mentioned in Tsimplis and Woodworth (1994), a 5 year-long segment can provide stable amplitudes and phase lags because it minimizes the large variability of annual and semi-annual calculated from each year. Therefore the harmonic analysis of mean monthly sea level anomaly will be based on 5 year averages of the time series.

Monthly sea level anomaly of stations in the GOT (Rayong, Phrachulachomkloa, Ko Lak, and Geting) and Andaman Sea (Ko Taphoa Noi and Langkawi) are shown in Fig. 8. Results from the harmonic analysis of all 14 stations are shown in Table 2 (note that Sattahip and Hua Hin records were too short to show the 5-year confidence intervals). The seasonal sea level signals found in the GOT and Andaman Sea are totally different with opposite phase, although they are influenced by similar meteorological conditions, such as monsoonal winds and air pressure. This suggests that the dynamic is influenced by wind-driven set-up processes — when wind is blowing from the east/west one expects set-up/set-down on the GOT/Andaman Sea coasts, leading to an opposite signal in sea level. In the GOT, the minimum sea level is observed around June–July and the maximum is found at the beginning/end of the year. However, in the Andaman Sea there are one minimum and two maxima. The minimum is found around February while the first and the second maximum are found around May–June and November, respectively.

The results of the harmonic analysis show that the annual amplitudes can be grouped into 3 categories: (1) the upper and eastern GOT, (2) the central and southern GOT (Ko Lak, Ko Mattaphon, and Geting), and (3) the Andaman Sea. In the upper and eastern GOT, the amplitude of S_a is in the range of 120 to 180 mm. In the central and southern GOT area, annual amplitude is found to be in the range of 200–240 mm. These two groups are similar to what have been shown by Tsimplis and Woodworth (1994), which mentioned that the annual amplitude in the GOT and Eastern Malaysian coasts are larger than 120 mm. The annual amplitudes found in the upper GOT and central GOT decrease toward the north. In the Andaman Sea, the annual amplitude is quite small compared with the one found in the GOT, ~100 mm at both Ko Taphoa Noi and Langkawi stations. Note that this value is approximately half that found at neighboring stations, Ko Mattaphon and Geting, but these stations are situated on the other side of the peninsula. In all stations the annual amplitude is several orders of magnitude larger than the astronomical global tidal equilibrium value, so the annual cycle is clearly not strictly an astronomical in nature, but most likely a wind-driven one. The semi-annual observed amplitude on the other hand is only slightly larger (~50%) than the global tidal value in the GOT, but ~3 times larger than the global value in the Andaman Sea.

Tsimplis and Woodworth (1994) stated that generally the magnitude of the annual amplitude is much larger than that of the semi-annual. In this study, the semi-annual amplitude is much smaller (~4 times) than the annual amplitude in the GOT, but in the Andaman Sea the amplitudes of S_a and S_{sa} are comparable. In the GOT, the semi-annual amplitude is in the range of 20 to 40 mm (Geting is an exception at 51 mm), but in the Andaman Sea the amplitude is ~60 mm. The semi-annual phase in the GOT increases toward the north, so that at Geting the maximum peak occurs ~1 month earlier than in the north. The peak is almost 3 months earlier at Bang Pakong station, where both annual and semi-annual amplitudes are small compare to other stations.

River discharge and thermal water expansion may have only small impact on seasonal sea level in this region. The peak of sea surface

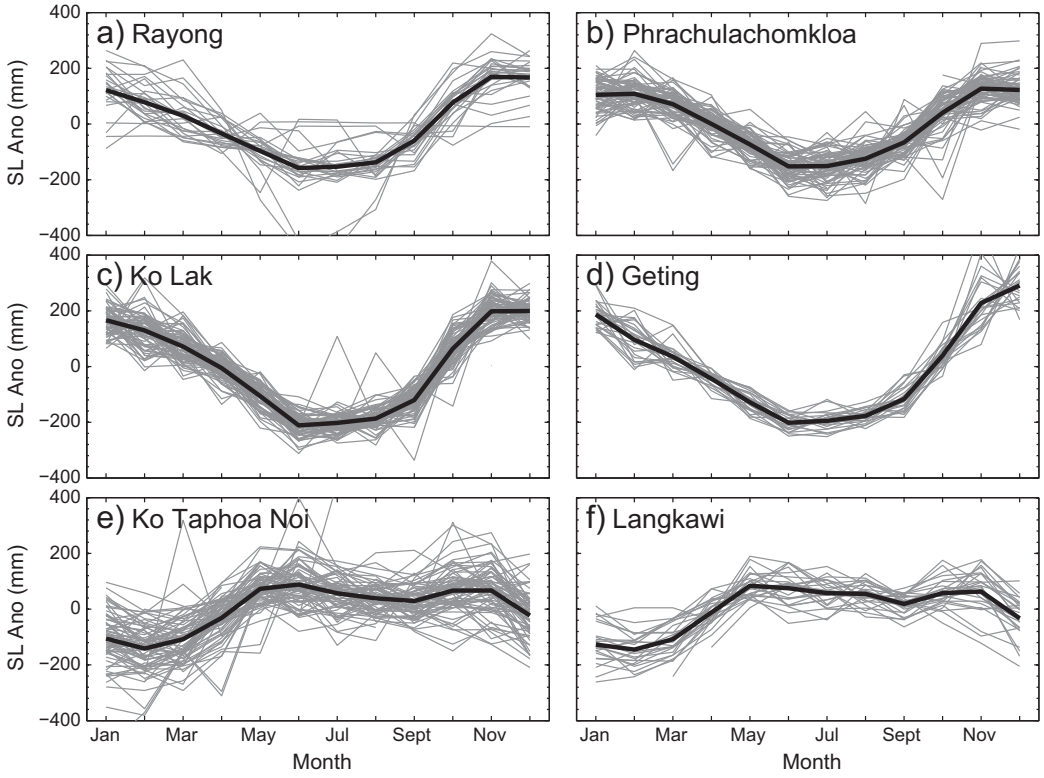

Fig. 8. Seasonal sea level cycle at stations in the GOT (a–d) and in the Andaman Sea (e–f). A black thick and gray thin lines represent mean monthly sea level anomaly and sea level anomalies for each year, respectively.

Table 2
Amplitudes (A) in mm and phase lags ($\varnothing$) in month of the maximum sea level from January ±95% confidence level of annual (S_a) and semi-annual (S_{sa}) sea level obtained from harmonic analysis at 14 tide gauge stations. The values are averages over 5-year periods; confidence level is not shown for 2 stations with too short records.

Station	A_{Sa} (mm)	A_{Ssa} (mm)	$\varnothing_{Sa}$ (mon)	$\varnothing_{Ssa}$ (mon)
Gulf of Thailand				
Rayong	170.06 ± 49.99	34.74 ± 18.09	−0.08 ± 0.39	−1.59 ± 0.76
Sattahip	177.88	15.83	0.39	−1.90
Si Chang	174.18 ± 12.09	28.28 ± 7.84	0.29 ± 0.11	−0.86 ± 1.35
Bang Pakong	122.80 ± 11.30	20.08 ± 7.60	−0.02 ± 0.17	−2.75 ± 0.41
Phrachulachomkloa	145.86 ± 8.36	27.08 ± 5.17	0.23 ± 0.06	−1.83 ± 0.81
Tha Chin	164.42 ± 33.95	33.05 ± 12.57	0.18 ± 0.12	−1.82 ± 0.41
Mae Klong	166.39 ± 20.12	20.90 ± 14.67	0.38 ± 0.40	−1.11 ± 1.44
Ban Lam	167.26 ± 34.81	39.61 ± 37.77	0.17 ± 0.59	−1.38 ± 1.75
Hua Hin	207.96	32.27	0.03	−1.96
Ko Lak	215.61 ± 9.98	38.87 ± 5.66	0.17 ± 0.05	−1.73 ± 0.16
Ko Mattaphon	239.77 ± 31.03	35.51 ± 12.10	0.12 ± 0.26	−1.35 ± 0.44
Geting	225.80 ± 13.00	51.51 ± 16.52	−0.03 ± 0.08	−1.00 ± 0.21
Andaman Sea				
Ko Taphoa Noi	97.68 ± 14.05	64.06 ± 7.69	−4.58 ± 0.23	−1.38 ± 0.17
Langkawi	97.08 ± 20.31	62.00 ± 9.27	−4.76 ± 0.13	−1.49 ± 0.18

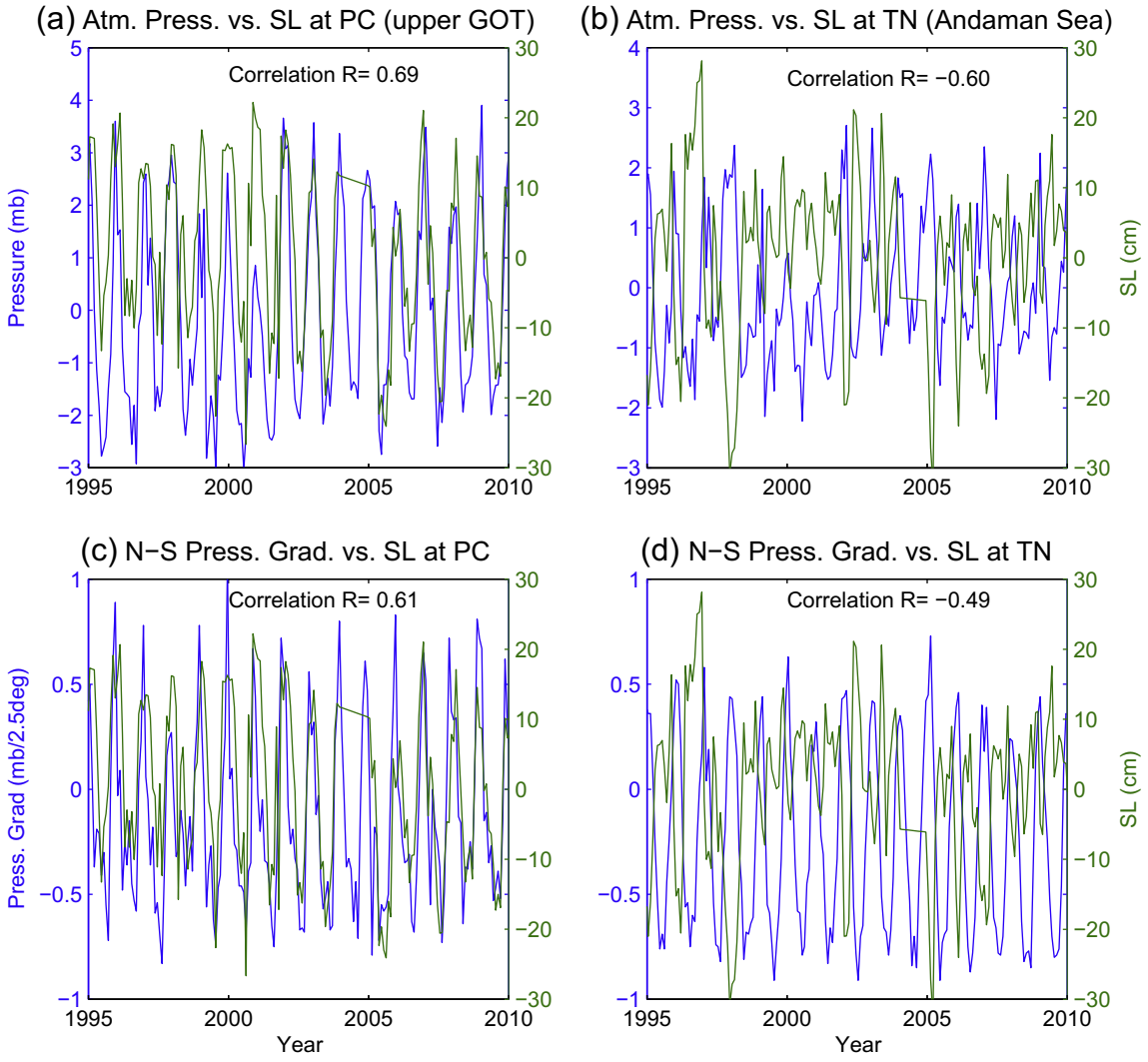

Fig. 9. Comparisons between monthly sea level anomalies (green lines; axis on the right) and atmospheric pressure (blue lines; axis on the left). Upper panels compare sea level at stations (a) PC (upper GOT) and (b) TN (Andaman Sea) with local atmospheric pressure, and bottom panels, c and d, compare the same two stations with the north–south pressure gradient over each station. The pressure gradient is the difference in pressure over 2.5° latitudes, which is proportional to the zonal wind; positive values represent wind coming from the east. Time-mean and linear trends were removed from all records. Correlation coefficients are shown (all have confidence level over 99%). (For interpretation of the references to color in this figure legend, the reader is referred to the web version of this article.)

temperature and water discharge are in April and October (major event) and June (minor event) (Singhrattna et al., 2005) with no significant correspondence in sea level. Moreover, because of the location of the GOT in low latitudes, seasonal sea surface temperature variations are very small (Saramul and Ezer, 2014) relative to mid-latitudes, with consequently very small thermal steric effect. Note that the mean seasonal sea level variation in the GOT, ~50 cm (e.g., between January and June at Ko Lak), is about one order of magnitude larger than the mean seasonal steric sea level variation at that latitude (~5 cm; Chen et al., 2000) and about 3 times larger than the global satellite-observed seasonal variations (~15 cm; Lombard et al., 2007).

The impact of atmospheric pressure on sea level can be seen in two ways, as a direct "invert barometer effect", and as a pressure gradient effect, representing wind-driven influence. Monthly sea level and monthly sea level atmospheric pressure anomalies at Phrachulachomkloa (GOT) and Ko Taphoa Noi (Andaman Sea) are shown in the upper panels of Fig. 9, while the sea level is compared with north–south pressure gradient in the lower panels of Fig. 9. Sea level pressure data is retrieved from http://iridl.ldeo.columbia.edu/. It is obtained from the Climate Data Assimilation System I; NCEP-NCAR Reanalysis Project (Kalnay et al., 1996). Sea level anomaly is highly correlated (over 99% confidence level) with both, local pressure and pressure gradient, but correlation coefficients are positive in the GOT and negative in the Andaman Sea. The direct impact of pressure on sea level (the invert barometer effect) implies that for each millibar (mb) increase in atmospheric pressure, sea level should drop by about 1 cm. However, the observed variations in sea level are ~10 times larger than the invert barometer impact (Fig. 9a, b) and in the GOT sea level *increases* with pressure, so we conclude that this is not a major driver for seasonal sea level variability. However, the pressure gradient comparisons (Fig. 9c, d) suggest that seasonal sea level variations are largely controlled by the seasonal wind pattern associated with the monsoon. Positive northward pressure gradient implies easterly winds (mostly in winter) that will cause sea level set-up in the GOT (i.e., positive pressure gradient–sea level correlation) and sea level set-down in the Andaman Sea (i.e., negative correlations), exactly as found here. The amplitude of sea level set-up can be estimated by $\Delta\eta \approx (L\tau) / (\rho g H)$, where L is a length scale, τ is the wind stress, g is the gravitational constant, ρ is the water density and H is the water depth near the coast (Csanady, 1982). For the GOT with L ~ 100 km, H ~ 10 m and monsoonal winds of ~7 m s^{-1} (Saramul and Ezer, 2014), the estimated sea level variations are $\Delta\eta \approx \pm 10$ cm, quite similar to the observed variations. Sea level set-up estimates in other shallow basins, such as in the Gulf of Carpentaria, also show good agreement with observations (Oliver and Thompson, 2010).

The seasonal sea level pattern in the GOT and Andaman Sea (Fig. 8) is thus consistent with monsoon-driven influence, as suggested by Punpuk (1981) and Sojisuporn et al. (2013). The results of the numerical simulations of the GOT by Oliver (2014) further support the idea of wind-driven coastal sea level setup, and the fact that the entire GOT is similarly affected by the large-scale wind pattern. During the southwest monsoonal winds, the sea level is piled against the coast (set-up) in the Andaman Sea, while water is pushed away from the coast (set-down) in the low GOT. However, during the northeast winter monsoon water in the Andaman Sea is pushed away from the Thailand coast, resulting in low sea level there, while water is transported from the South China Sea into the GOT, resulting in high water levels throughout the GOT. The seasonal sea level pattern in the upper GOT is similar to that found in the lower GOT, indicating that it is a large-scale pattern, not a local phenomenon. In the Andaman Sea, apart from monsoonal winds, the movement of coastally-trapped waves might also affect sea level (Brown, 2007), as well as ocean–atmosphere–land interactions associated with the El Nino and La Nina events (Webster et al., 1999). The somewhat smaller correlations and more complex pattern of pressure and sea level in the Andaman Sea (Fig. 9b, d), compared with the GOT (Fig. 9a, c), may indicate influences from additional sources other than the seasonal monsoonal wind.

4. Conclusions

Sea level data in the GOT and the Andaman Sea obtained from several different local sources (MD) and global archives (PSMSL and UHSLC) are used to study two aspects of coastal sea level: (1) sea level rise and its spatial variation due to land subsidence, and (2) seasonal variations of sea level along the coasts of Thailand. The study analyzed more extensive sea level data than most previous studies of the region. To study the first aspect, RSLR was calculated from two different methods, a standard linear regression and a non-linear HHT/EMD method (following recent studies of sea level trends; Ezer and Corlett, 2012; Ezer, 2013; Ezer et al., 2013). The average rate of RSLR along the coasts of Thailand is around 6 mm y^{-1} in both method analyses, but the analyses also show very significant spatial pattern in RSLR associated with land motion. However, there are insufficient data over land to describe the spatial variations in geological-, hydrological- and seismic-related subsidence, so the best estimates of land movement are obtained from the difference between the global sea level rise and the RSLR shown in Fig. 4. It is clear from these results that RSLR in this region is dominated by regional land movement over the smaller global sea level rise. The faster rates, ~10–20 mm y^{-1}, or ~5–10 times greater than mean rates from global tide gauges (Church and White, 2006, 2011), were found at Phrachulachomkloa, Tha Chin, Mae Klong, and Ban Lam, where groundwater extraction causes significant land subsidence. This has important consequences for the population of Bangkok and surrounded area. Vertical land movement as a result of continuous seismic activity is also contributing to RSLR in Thailand (Trisirisatayawong et al., 2011), as is the vertical land movement following the December 2004 Sumatra–Andaman Earthquake (Satirapod et al., 2013). Therefore estimating rate of sea level rise in Thailand is tricky and it must take vertical land movement into consideration; moreover, RSLR rates are not stationary, but sometimes rapidly changing with land movements due to groundwater extraction (Gornitz, 2001) and earthquakes (Sieh et al., 2008). Our analysis indicates much higher rates, ~19–34 mm y^{-1} after the 2004 earthquake in all stations, indicating RSLR acceleration that is much larger than global acceleration (Church and White, 2011; Dean and Houston, 2013) or even regional acceleration along the U.S. East Coast (Ezer and Corlett, 2012; Ezer, 2013; Kopp, 2013). However, while global changes in coastal sea level rise is associated with changing rates of thermal expansion and land ice melting, and regional changes may be associated with climatic shift in ocean currents (Sallenger et al., 2012; Ezer et al., 2013), in the GOT most of the change in RSLR is contributed by changes in land movements. An interesting result is that after the 2004 earthquake the high RSLR rates are much more even in the GOT, relative to more pronounced spatial variations before the 2004 earthquake. However, the period after the earthquake is less than 10 years, so longer observations are needed before conclusive results are obtained about the persistent of the high rates into the future.

As for the second aspect of this study, the seasonal variations were analyzed for many more tide gauge stations than in past studies (e.g., Tsimplis and Woodworth, 1994), and forcing from several sources were considered. The most interesting result is how different the annual and semi-annual signals are, even for neighboring stations, if one is located on the GOT side and one on the Andaman Sea side of the coast. In general, the annual sea level signal is dominant over the semi-annual signal in the GOT, while in the Andaman Sea the annual and semi-annual signals are more comparable in amplitude. The amplitudes of annual signal in the GOT are in the range of 120 to 240 mm which is approximately 5 times greater than semi-annual signal. In the Andaman Sea, the annual signal is approximately 2 times greater than the semi-annual signal (annual amplitude is ~ 100 mm). The latter result could be explained by the fact that the observed semi-annual cycle in the region is largely driven by the long-term astronomical semi-annual cycle, while the annual cycle is mostly driven by the seasonal monsoonal wind and atmospheric pressure patterns. The comparison between monthly mean sea level anomaly and sea level pressure

shows positive and negative correlations for stations in the GOT and Andaman Sea, respectively. It seems that large scale monsoonal winds (represented here by atmospheric pressure gradients, Fig. 9c, d) are responsible for the annual cycle. For example, during the early summer, monsoonal winds from the southwest pile up waters on the Andaman Sea coast and causing high sea level in May–June, while during the winter, monsoonal winds from the northeast transport waters from the South China Sea toward the GOT and causing maximum sea level there in January. It is interesting to note that the wind-driven mechanism of seasonal sea level variability associated with the monsoonal winds seen here is consistent with a similar mechanism that drives intraseasonal sea level variations associated with the MJO (Oliver, 2014). The seasonal peak-to-peak seasonal sea level change in the GOT is much larger than most other coastal locations, and about 10 times larger than thermal steric effects at that latitude (Chen et al., 2000), so together with sea level rise, seasonal variations cannot be neglected when considering flooding risks, coastal erosion and other environmental hazards in the region.

Acknowledgments

This study is part of S. Saramul's graduate studies at Old Dominion University (ODU). Support from ODU's Department of Ocean, Earth and Atmospheric Sciences (OEAS), including Dorothy Brown Smith Scholarship, and from the computational resources of the Center for Coastal Physical Oceanography (CCPO) are acknowledged. Additional support is provided by the Thai Government Science and Technology scholarship and from Chulalongkorn University. T. Ezer was partly supported by grants from the NOAA Climate Programs, the Kenai Peninsula Borough, Alaska, and ODU's Climate Change and Sea Level Rise Initiative (CCSLRI). The authors would like to thank the Marine Department of Thailand, PSMSL, and UHSLC for providing sea level data. Reviewers are thanked for many suggestions that greatly helped to improve the manuscript.

References

Aobpaet, A., Cuenca, M.C., Hooper, A., Trisirisatayawong, I., 2009. Land subsidence evaluation using InSAR time series analysis in Bangkok metropolitan area. In: Lacoste-Francis, H. (Ed.), Proc. of 'Fringe 2009' ESRIN, Frascati, Italy (ESA SP-677, March 2010). ESA Communications, Noordwijk, The Netherlands.

Aschariyaphotha, N., Wongwises, P., Wongwises, S., Humphries, U., You, X., 2008. Simulation of seasonal circulations and thermohaline variabilities in the Gulf of Thailand. Adv. Atmos. Sci. 25 (3), 489–506. http://dx.doi.org/10.1007/s00376-008-0489-3.

Brown, B.E., 2007. Coral Reefs of the Andaman Sea — An Integrated Perspective. In: Gibson, R.N., Atkinson, R.J.A., Gordon, J.D.M. (Eds.), Oceanogr. Mar. Biol. Annual Review. vol. 45. CRC Press, Florida, pp. 173–194. http://dx.doi.org/10.1201/9781420050943.ch5.

Chen, J.L., Shum, C.K., Wilson, C.R., Chambers, D.P., Tapley, B.D., 2000. Seasonal sea level change from TOPEX/Poseidon observation and thermal contribution. J. Geodesy 73 (12), 638–647. http://dx.doi.org/10.1007/s001900050002.

Church, J.A., White, N.J., 2006. A 20th century acceleration in global sea-level rise. Geophys. Res. Lett. 33, L01602. http://dx.doi.org/10.1029/2005GL024826.

Church, J.A., White, N.J., 2011. Sea-level rise from the late 19th century to the early 21st century. Surv. Geophys. 32, 585–602. http://dx.doi.org/10.1007/s10712-011-9119-1.

Csanady, G.T., 1982. Circulation in the Coastal Ocean. Vol. 2. Springer, p. 279.

Dean, R.J., Houston, J.R., 2013. Recent sea level trends and accelerations: comparison of tide gauge and satellite results. Coast. Eng. 74, 4–9.

Douglas, B.C., 2001. An introduction to sea level. In: Douglas, B.C., Kearney, M.S., Leatherman, S.P. (Eds.), Sea-level Rise: History and Consequences. Academic Press, California, pp. 1–11.

Dura, T., Rubin, C.M., Kelsey, H.M., Horton, B.P., Hawkes, A., Vane, C.H., Daryono, M., Pre, C. G., Ladinsky, T., Bradley, S., 2011. Stratigraphic record of Holocene coseismic subsidence, Padang, West Sumatra. J. Geophys. Res. Solid Earth 116 (B11). http://dx.doi.org/10.1029/2011JB008205.

Ezer, T., 2013. Sea level rise, spatially uneven and temporally unsteady: why the U.S. East Coast, the global tide gauge record and the global altimeter data show different trends. Geophys. Res. Lett. 40 (20), 5439–5444. http://dx.doi.org/10.1002/2013GL057952.

Ezer, T., Corlett, W.B., 2012. Is sea level rise accelerating in the Chesapeake Bay? A demonstration of a novel new approach for analyzing sea level data. Geophys. Res. Lett. 39, L19605. http://dx.doi.org/10.1029/2012GL053435.

Ezer, T., Atkinson, L.P., Corlett, W.B., Blanco, J.L., 2013. Gulf Stream's induced sea level rise and variability along the U.S. mid-Atlantic coast. J. Geophys. Res. 118 (2), 685–697. http://dx.doi.org/10.1002/jgrc.20091.

Forbes, A.M.G., Church, J.A., 1983. Circulation in the Gulf of Carpentaria. II. Residual currents and mean sea levels. Mar. Freshw. Res. 34 (1), 11–22.

Fuh, Y., 1977. Theoretical Study of Tides in Gulf. (Ph.D. Thesis) Asian Institute of Technology, Bangkok, Thailand.

Gill, A.E., Niiler, P.P., 1973. The theory of the seasonal variability in the ocean. Deep Sea Res. 20 (2), 141–177.

Gornitz, V., 2001. Impounding, groundwater mining and other hydrological transformations: impact on global sea level rise. In: Douglas, B.C., Kearney, M.S., Leatherman, S.P. (Eds.), Sea-level Rise: History and Consequences. Academic Press, California, pp. 97–119.

Holgate, S.J., Matthews, A., Woodworth, P.L., Rickards, L.J., Tamisiea, M.E., Bradshaw, E., Foden, P.R., Gordon, K.M., Jevrejeva, S., Pugh, J., 2013. New data systems and products at the Permanent Service for Mean Sea Level. J. Coastal Res. 29 (3), 493–504. http://dx.doi.org/10.2112/JCOASTRES-D-12-00175.1.

Huang, N.E., Shen, Z., Long, S.R., Wu, M.C., Shih, E.H., Zheng, Q., Tung, C.C., Liu, H.H., 1998. The empirical mode decomposition and the Hilbert spectrum for non stationary time series analysis. Proc. R. Soc. Lond. 454, 903–995. http://dx.doi.org/10.1098/rspa.1998.0193.

Jevrejeva, S., Grinsted, A., Moore, J.C., Holgate, S., 2006. Nonlinear trends and multiyear cycles in sea level records. J. Geophys. Res. 111, C09012. http://dx.doi.org/10.1029/2005JC003229.

Kalnay, E., Kanamitsu, M., Kistler, R., Collins, W., Deaven, D., Gandin, L., Iredell, M., Saha, S., White, G., Woolen, J., Zhu, Y., Chelliah, M., Ebisuzaki, W., Higgins, W., Janowiak, J., Mo, K.C., Ropelewski, C., Wang, J., Reynolds, R., Jenne, R., Joseph, D., 1996. The NCEP/NCAR 40-year reanalysis project. Bull. Am. Meteorol. Soc. 77 (3), 437–471.

Kopp, R.E., 2013. Does the mid-Atlantic United States sea-level acceleration hot spot reflect ocean dynamic variability? Geophys. Res. Lett. 40, 3981–3985. http://dx.doi.org/10.1002/grl.50781.

Lombard, A., Garcia, D., Ramillien, G., Cazenave, A., Biancale, R., Lemoine, J.M., Flechtner, F., Schmidt, R., Ishii, M., 2007. Estimation of steric sea level variations from combined GRACE and Jason-1 data. Earth Planet. Sci. Lett. 254 (1), 194–202.

Nicholls, R.J., 2011. Planning for the impacts of sea level rise. Oceanography 24 (2), 142–155.

Oliver, E.C.J., 2014. Intraseasonal variability of sea level and circulation in the Gulf of Thailand: the role of the Madden–Julian Oscillation. Clim. Dyn. 42 (1–2), 401–416. http://dx.doi.org/10.1007/s00382-012-1595-6.

Oliver, E.C.J., Thompson, K.R., 2010. Madden–Julian Oscillation and sea level: local and remote forcing. J. Geophys. Res. 115, C01003. http://dx.doi.org/10.1029/2009JC005337.

Peltier, W.R., 2001. Global Glacial Isostatic Adjustment and modern instrument records of relative sea level history. In: Douglas, B.C., Kearney, M.S., Leatherman, S.P. (Eds.), Sea-level Rise: History and Consequences. Academic Press, California, pp. 97–119.

Peltier, W.R., 2004. Global glacial isostasy and the surface of the Ice-Age Earth: the ICE-5G (VM2) model and GRACE. Annu. Rev. Earth Planet. Sci. 32, 111–149.

Peltier, W.R., Luthcke, S.B., 2009. On the origins of earth rotation anomalies: new insight on the basis of both "paleogeodetic" data and Gravity Recovery and Climate Experiment (GRACE) data. J. Geophys. Res. 114, B11405. http://dx.doi.org/10.1029/2009JB006352.

Phien-Wej, N., Giao, P.H., Nutalaya, P., 2006. Land subsidence in Bangkok, Thailand. Eng. Geol. 82, 187–201. http://dx.doi.org/10.1016/j.enggeo.2005.10.004.

Poland, J.F., 1984. Guidebook to Studies of Land Subsidence Due to Ground-water Withdrawal (Tech. Rep.). UNESCO, Michigan.

Punpuk, V., 1981. Sea Level Variation in Gulf of Thailand. (Master's Thesis) Naval Postgraduate School, California, USA, (149 pp.).

Rizal, S., Damm, P., Wahid, M.A., Sundermann, J., Ilhamsyah, Y., Iskandar, T., Muhammad, 2012. General circulation in the Malacca Strait and Andaman Sea: a numerical model study. Am. J. Environ. Sci. 8, 479–488. http://dx.doi.org/10.3844/ajessp.2012.479.488.

Sallenger, A.H., Doran, K.S., Howd, P., 2012. Hotspot of accelerated sea-level rise on the Atlantic coast of North America. Nat. Clim. Chang. 2, 884–888. http://dx.doi.org/10.1038/NCILMATE1597.

Saramul, S., 2013. Observations and Modeling Forcing Mechanisms for the Coastal Dynamics of the Upper Gulf of Thailand. (Ph.D. Dissertation) Old Dominion University, (154 pp.).

Saramul, S., Ezer, T., 2014. On the dynamics of low latitude, wide and shallow coastal system: numerical simulations of the Upper Gulf of Thailand. Ocean Dyn. 64, 557–571. http://dx.doi.org/10.1007/s10236-014-0703-z.

Satirapod, C., Trisirisatayawong, I., Fleitout, L., Garaud, J.D., Simons, W.J.F., 2013. Vertical motions in Thailand after the 2004 Sumatra–Andaman Earthquake from GPS observations and its geophysical modeling. Adv. Space Res. 51, 1,565–1,571. http://dx.doi.org/10.1016/j.asr.2012.04.030.

Sieh, K., Natawidjaja, D.H., Meltzner, A.J., Shen, C.C., Cheng, H., Li, K.S., Suwargadi, B.W., Galetzka, J., Philibosian, B., Edwards, R.L., 2008. Earthquake supercycles inferred from sea-level changes recorded in the corals of West Sumatra. Science 322 (5908), 1674–1678. http://dx.doi.org/10.1126/science.1163589.

Singhrattna, N., Rajagopalan, B., Krishna Kumar, K., Clark, M., 2005. Interannual and interdecadal variability of Thailand summer monsoon season. J. Clim. 18, 1,697–1,708. http://dx.doi.org/10.1175/JCLI3364.1.

Siwapornnanan, C., Humphries, U.W., Wongwises, P., 2011. Characterization of the observed sea level and sea surface temperature in the Gulf of Thailand and the South China Sea. Appl. Math. Sci. 5 (27), 1,295–1,305.

Sojisuporn, P., Sangmanee, C., Wattayakorn, G., 2013. Recent estimate of sea-level rise in the Gulf of Thailand. Maejo Int. J. Sci. Technol. 7, 106–113.

Syvitski, J.P., Kettner, M., Overeem, A.J., Hutton, I., Hannon, E.W.H., Brankenridge, M.T., Day, G.R., Voeroesmarty, J., Saito, C., Giosan, Y.L., Nicholls, R.J., 2009. Sinking deltas due to human activities. Nat. Geosci. 2, 681–686. http://dx.doi.org/10.1038/NGEO629.

Therakomen, S., 2001. Water Community Revitalization: An Urban Design Project for Supporting the Use of Waterways in Modern Bangkok. (Master's Thesis) Univ. of Washington, Washington.

Torres, R.R., Tsimplis, M.N., 2012. Seasonal sea level cycle in the Caribbean Sea. J. Geophys. Res. 117, C07011. http://dx.doi.org/10.1029/2012JC008159.
Trisirisatayawong, I., Naeije, M., Simons, W., Fenoglio-Marc, L., 2011. Sea level change in the Gulf of Thailand from GPS-corrected tide gauge data and multi-satellite altimetry. Global Planet. Chang. 76, 137–151. http://dx.doi.org/10.1016/j.gloplacha.2010.12.010.
Tsimplis, M.N., Woodworth, P.L., 1994. The global distribution of the seasonal sea level cycle calculated from coastal tide gauge data. J. Geophys. Res. 99 (C8), 16,031–16,039. http://dx.doi.org/10.1029/94JC01115.
Vongvisessomjai, S., 2006. Will sea-level really fall in the Gulf of Thailand? Songklanakarin J. Sci. Technol. 28 (2), 227–248.
Vongvisessomjai, S., 2010. Effect of global warming in Thailand. Songklanakarin J. Sci. Tech. 32 (4), 431–444.
Webster, J.P., Moore, A.M., Loschnigg, J.P., Leben, R.R., 1999. Coupled ocean–atmosphere dynamics in the Indian Ocean during 1997–98. Nature 401, 356–360. http://dx.doi.org/10.1038/43848.
Woodworth, P.L., Player, R., 2003. The permanent service for mean sea level: an update to the 21st century. J. Coastal Res. 19 (2), 287–295.
Wu, C.-R., Shaw, P.-T., Chao, S.-Y., 1998. Seasonal and interannual variations in the velocity field of the South China Sea. J. Oceanography 54 (4), 361–372. http://dx.doi.org/10.1007/BF02742620.
Wyrtki, K., 1961. Scientific results of marine investigations of the South China Sea and the Gulf of Thailand 1951–1961: physical oceanography of the South East Asian Waters. Naga Report. Vol. 2. The University of California, Scripps Institute of Oceanography, La Jolla, CA (195 pp.).
Yanagi, T., Akaki, T., 1994. Sea level variation in the Eastern Asia. J. Oceanogr. 50, 643–651.
Yi-Neng, L., Shi-Qiu, P., Xue-Zhi, Z., 2012. Observations and simulations of the circulation and mixing around the Andaman–Nicobar Submarine Ridge. Atmos. Ocean. Sci. Lett. 5 (4), 319–323.